

Transport studies for Wendelstein 7-X

O. Grulke^{1,2}, J.H. Proll¹, P. Xanthopoulos¹, T. Windisch¹ and G. Weir¹

¹MPI for Plasma Physics, Greifswald, Germany

²Department of Physics, Technical University of Denmark, Lyngby, Denmark

Corresponding Author: grulke@ipp.mpg.de

Abstract:

Turbulent transport is investigated for realistic magnetic field geometry and plasma profiles in Wendelstein 7-X. The key instabilities under consideration are trapped electron modes (TEM) and the ion temperature gradient instability (ITG). The TEM instability mechanism as a resonant process between drift wave fluctuation and the precession of electrons trapped in a magnetic well is studied by analysis of bad magnetic curvature regions and local magnetic wells. It is shown that the TEM instability varies when different magnetic configurations are considered. ITG turbulence is studied on the basis of fully nonlinear flux-surface simulations. The ITG fluctuation amplitude is strongly localized in regions of bad magnetic curvature. It has an amplitude envelope along the magnetic field and smaller amplitudes are observed where the local magnetic shear is large. It is discussed to what extent the set of dedicated core fluctuation diagnostics is able to test experimentally the theoretical results.

1 Introduction

A major issue of stellarators has been the increased level of neoclassical transport when compared to tokamaks. Modern stellarator designs seek for configurations favorable with respect to transport by tailoring the magnetic field geometry towards quasi-symmetry or, in the case of W7-X, quasi-isodynamicity. It has indeed been shown that the neoclassical transport can be reduced to the tokamak level [1]. Wendelstein 7-X (W7-X) stands in this line and theoretical and first experimental results indicate that neoclassical transport is reduced. However, none of the optimization criteria of W7-X (or any other stellarator) included any optimization of turbulent transport which, after the neoclassical transport reduction, will play a major role in the confinement properties. This is mainly due to a lack of understanding and numerical simulation tools of microturbulence in realistic three-dimensional stellarator geometry. Over the last decade, tremendous progress has been made in modeling and simulation of stellarator turbulence to a level that detailed comparisons between theoretical/simulation results and experiments can be performed [2]. Although the magnetic field geometry of stellarators, particularly W7-X, differs strongly from the tokamak situation, the same types of microinstabilities are discussed to be responsible for the turbulent transport. Similar to tokamaks, trapped electron modes (TEM)

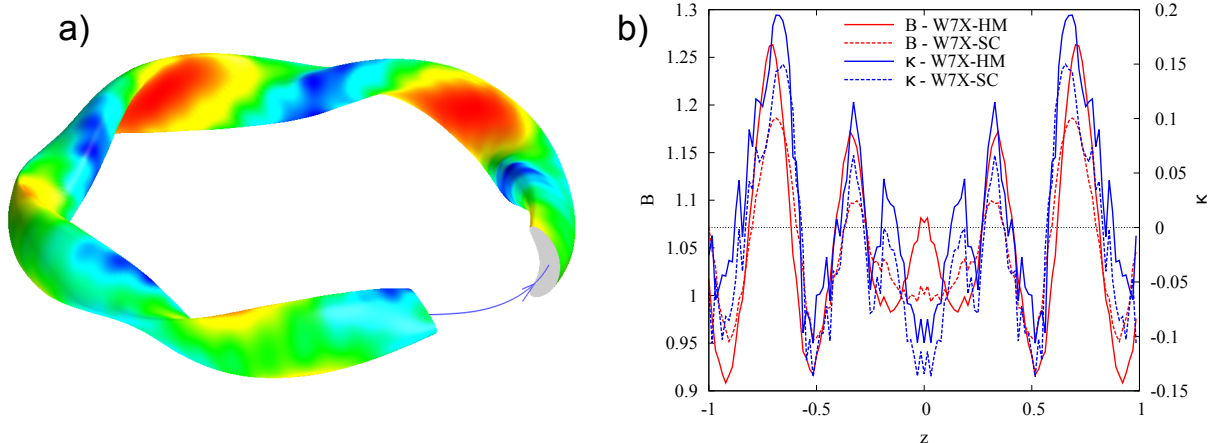


FIG. 1: a) Color-coded magnetic field strength on a magnetic flux surface for the W7-X standard configuration. Red denotes high, blue low magnetic field. b) Comparison of the magnitude of the magnetic field B and local curvature κ along a magnetic flux tube for the high mirror (HM) and the standard magnetic field configuration (SC). Negative values $\kappa < 0$ correspond to bad curvature, $z = 0$ denotes the outboard midplane.

and the ion temperature gradient instability (ITG) are expected to play an important role in turbulent transport processes. In this paper we concentrate on the studies of the evolution of ion temperature gradient (ITG) and trapped electron modes (TEM) in W7-X. Fundamental linear instability estimates for TEM and nonlinear simulations using the GENE code for ITG turbulence are used. These studies are done for realistic plasma parameter profiles based on neoclassical transport calculations and W7-X specific magnetic field geometries. An important aspect of the investigation is to what extent key features of the turbulence can be observed and identified with the set of dedicated fluctuation diagnostics available in the next W7-X operation phase.

2 TEM instability

The TEM instability is essentially a drift wave driven by the radial plasma density gradient and destabilized by density perturbations of electrons being trapped in a magnetic well. Thus, the TEM is fundamentally expected to become unstable in regions of bounce-averaged bad magnetic curvature, where a resonance of the drift wave phase velocity and the precessional drift of trapped electrons exist. In tokamaks, this region is generally located on the outboard midplane and TEM have been observed here in the case of peaked radial plasma density gradients. However, in stellarators the situation must be analyzed for the specific magnetic field geometry. It has been shown that in the limiting case of a quasi-isodynamic stellarator (maximum-J configuration), all particles experience good average curvature and the TEM is widely stable [3]. The analysis of the magnetic curvature and trapping region is taken in this paper as a worst case estimate for TEM instability. Influences on the trapped electron density, as, e.g., collisional de-trapping,

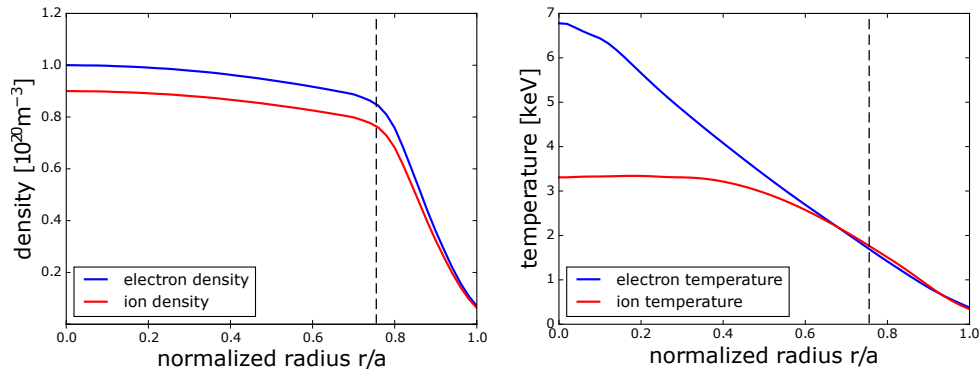


FIG. 2: Plasma density and temperature profiles as obtained from neoclassical estimates. The vertical dashed line indicated the flux surface chosen for the simulation runs.

are not considered. The magnetic field geometry of W7-X only approaches a quasi-isodynamic configuration. Fig. 1a) shows the distribution of magnetic field strength on a single magnetic flux surface for one standard configuration. Regions of low magnetic field that correspond to regions of trapped particles and potential TEM instability are colored in blue and are located mainly close to the triangular cross-section in each of the five symmetric modules. In W7-X those regions are not only located on the outboard side as for a tokamak, but wrap around poloidally. The regions of high magnetic field, colored in red, are found in the bean-shaped regions and here TEM is expected to be more stable. The flexibility of the magnetic field configuration allows to tune into different situations with respect to the TEM stability, as is depicted in Fig. 1b). Here the so-called standard configuration (SC) is compared to the high-mirror configuration (HM). Shown are the magnetic field strength and local magnetic curvature along a magnetic flux tube at half minor radius and crossing the outboard midplane $z = 0$. At this position a major difference between the two configurations is found: In the SC the magnetic well overlaps with the region of bad curvature, whereas in the HM configuration the bad curvature remains but the magnetic field shows a local maximum here. Thus, the TEM is expected to be more stable in this configuration. This is indeed observed in linear gyrokinetic simulations performed with the GENE code: For gradients hinting at a more density-gradient-driven TEM, the HM configuration has lower growth rates than the SC, especially in the transport-relevant large scales (low wave numbers) [4].

3 ITG turbulence

As for the TEM, the ITG is another drift wave-type instability. It is driven by the radial ion temperature gradient, which leads to gradients of poloidal ion drifts and instability growth due the resulting plasma potential perturbations and associated radial $E \times B$ drifts. In contrast to the standard drift wave instability mechanism, the ITG mode can become unstable even in the case of adiabatic electrons. The nonlinear evolution of the ITG instability for W7-X is studied for the standard case magnetic configuration for

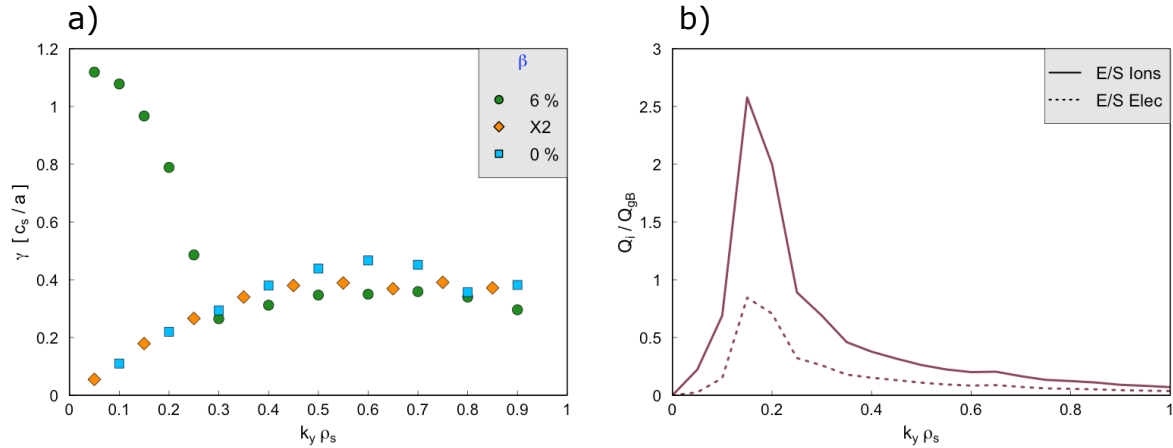


FIG. 3: a) Binormal spectrum of the linear growth rate for kinetic ballooning modes (green circles) and ITG for the X2 heating scenario under consideration (orange diamonds) and a zero- β plasma case (blue squares). b) Wavenumber spectrum of the electrostatic heat transport contribution of electrons and ions for the X2 heating scenario.

plasma parameter profiles depicted in Fig. 2. These are estimates based on neoclassical transport for a central ECRH heating power of 5 MW in X2 polarization. An effective charge state $z_{eff} = 1.5$ is assumed. The plasma density is moderate in the range $n \leq 1 \cdot 10^{20} \text{m}^{-3}$. The main radial density gradient region is located in the last 20% of the minor radius. At these relatively low densities the coupling between electrons and ions in the plasma center is rather weak and ions are typically a factor of two colder than the electrons, which have a peak temperature of $T_e \approx 7 \text{keV}$. Those values are realistic and have been readily achieved in the first operation phase. The central plasma is dominated by electron root confinement and consequently the radial electric field is positive. The main ion temperature gradient region spans over half of the outer minor radius. For this situation GENE full flux surface simulations have been performed. The flux surface chosen is located at $r/a = 0.75$ as indicated by the vertical dashed lines. The electrons are adiabatic and thus fluctuation amplitudes are expressed as plasma potential fluctuation amplitudes. The radial electric field is neglected for the present simulations. The growth rates extracted from the simulation run are shown in Fig. 3a). The X2 heating scenario shows the linear growth of ITG over a rather broad wavenumber range $k\rho_s = 0.1 - 1$ (ρ_s denotes the ion gyroradius). The result is very similar to the zero plasma- β case and only in the ITG branch small deviations are visible. For comparison an additional case is shown, suggesting that, in W7-X, the kinetic ballooning mode generally appears only at very large beta values ($\beta = 6\%$ shown here). The resulting ITG turbulence does indeed cause strong turbulent heat transport, as shown in Fig. 3b). The transport is predominantly caused by electrostatic ITG turbulence with the electromagnetic contribution being apparently an order of magnitude smaller. The transport peaks in the low wavenumber range indicating the importance of small-scale turbulent eddies to the transport. Importantly, when kinetic electrons are considered in the simulations, the ion contribution to the transport is much

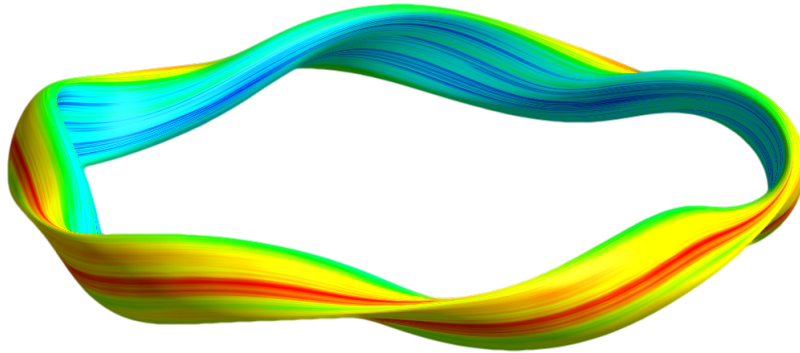


FIG. 4: Color-coded rms amplitude of ITG potential fluctuations obtained by GENE simulations of the scenario depicted in Fig. 2.

larger than the electron contribution. In contrast to tokamak ITG turbulence, where large fluctuation amplitudes are found on the entire outboard side of the plasma in the region of bad magnetic curvature, the distribution in W7-X is much more structured as shown in Fig.4. Large fluctuation amplitudes are observed in a poloidally narrow strip predominantly on the outboard side. In poloidal direction the fluctuation amplitudes drop off rather quickly and have only low levels on the entire inboard side. The narrow strip of large amplitudes is located in a region of bad magnetic curvature, known to be a strong destabilizing factor for ITG turbulence. Thus, the distribution of amplitudes closely follows the W7-X magnetic field characteristics. Careful inspection reveals that the high amplitude region has an envelope along the magnetic field with a maximum in the bean shape cross section of the plasma and a decrease towards the triangular shaped cross section. This feature is not linked to a corresponding variation of bad curvature. Instead, it is mainly caused by the local magnetic shear. Fig. 5 compares the time-averaged fluctuation amplitude along a magnetic flux tube with the local magnetic shear. The amplitude envelope is clearly observed with a peak at the outboard midplane of the bean shaped cross section. The local magnetic shear displays a strong increase when following the flux tube towards the triangular cross section. This strong increase correlates with the decrease of fluctuation amplitude and does not only hold for the envelope of the fluctuation maximum but can also be observed all along the flux tube. This effect is well known from tokamak turbulence, which is driven predominantly on the outboard midplane and streams along the magnetic field towards the X-point. The strong local X-point magnetic shear leads to stretching of the turbulent eddies, effectively a modification of the wavenumber spectrum, which has been demonstrated to decrease the fluctuation amplitudes [5] and for sufficiently strong shear eventually leads to a de-correlation of the turbulent eddies. A similar effect is observed in the W7-X geometry, however not associated with a magnetic X-point but in the plasma volume. One could speculate that the associated transport asymmetry along the magnetic flux tube induces parallel plasma flows towards the triangular cross section. This aspect is under debate and requires further studies.

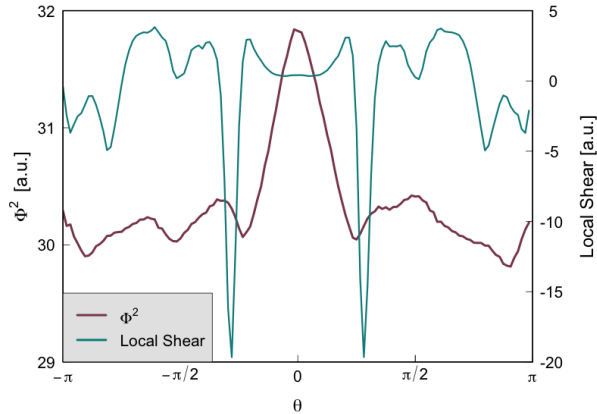


FIG. 5: RMS fluctuation amplitude Φ^2 and local magnetic shear along a magnetic flux tube. θ denotes the poloidal Boozer angle, used to parameterize the parallel direction.

4 Turbulence diagnostics

The simulation results demonstrate key qualitative properties, which can be addressed as a first step using the core fluctuation diagnostics envisaged to be available in OP 1.2. Fig. 6 gives an overview of the toroidal location and poloidal cross section of the magnetic field configuration for the diagnostics under consideration. The temporal resolution for all diagnostics is $f = 2 - 5$ MHz, while the wavenumber resolution is compiled in Tab. I. In total three reflectometer systems are available: Two Doppler reflectometer systems in modules M2 and M5 measure electron density fluctuations and the associated poloidal phase velocity in the outer density gradient region. Both are toroidally located in different cross sections. The measurement region of system in M2 is directly in the bean-shaped cross section at largest bad curvature and a toroidally localized local magnetic well, whereas the system in M5 is in between bean-shaped and triangular-shaped cross section, which has much less bad curvature but a much broader trapping magnetic field structure. Both systems provide a wavenumber resolution in the range $k_\theta \approx 10 \text{ cm}^{-1}$, corresponding to $k_\perp \rho_s \approx 1$ well in the range of the linear the TEM and ITG instability. Thus, already with these two systems qualitatively different regions are sampled, which will provide first indications, if indeed a strong localization of fluctuations in the bad curvature region is observed. Additionally, the important mechanism of turbulence transport reduction by the occurrence of zonal flows can be directly detected by fluctuation phase velocity measurements at two different locations on the same magnetic flux surface. The measurement of the localization of fluctuations in the bad curvature region is complemented by two correlation ECE systems, which are installed in M4&5 and measure electron temperature fluctuations in the good curvature region on the inboard plasma side. The wavenumber resolution is towards larger spatial fluctuation structures with $k_\perp \approx 3 - 5 \text{ cm}^{-1}$. According to the ITG simulation results ITG modes are nonlinearly stable and the fluctuation degree on the inboard side is small. The direct comparison between the good and bad

TABLE I: CHARACTERISTIC WAVENUMBER RESOLUTION OF THE W7-X CORE FLUCTUATION DIAGNOSTICS.

diagnostics (module)	wavenumber resolution [cm^{-1}]
Doppler reflectometer (M2)	$9 \leq k_\theta \leq 14$ (O-mode) $6 \leq k_\theta \leq 14$ (X-mode)
correlation ECE (M4)	$0.3 \leq k_r \leq 5$
Doppler reflectometer (M5)	$9 \leq k_\theta \leq 14$ (O-mode) $6 \leq k_\theta \leq 13$ (X-mode)
correlation ECE (M5)	$0.3 \leq k_\theta \leq 1$
phase contrast imaging (M5)	$1 \leq k_\theta \leq 30$

curvature region is provided by the simultaneous measurement of density fluctuations by

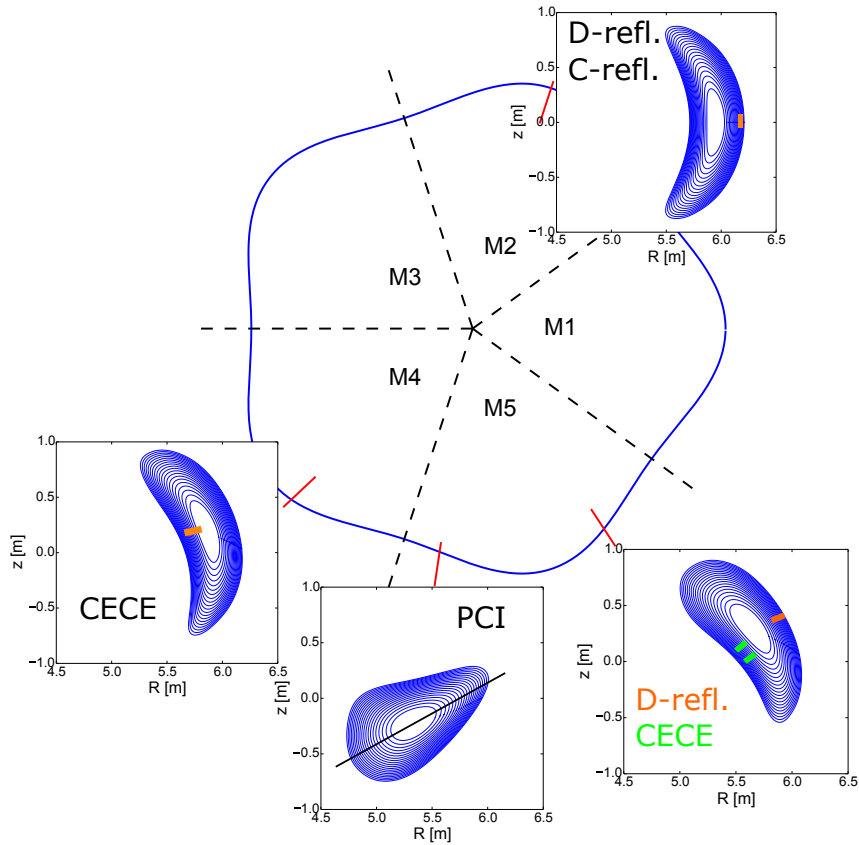


FIG. 6: Overview of toroidal location of fluctuation diagnostics and the respective poloidal cross-section of Doppler reflectometer (D-refl.), correlation reflectometer (C-ref.), phase contrast imaging (PCI) and correlation ECE (CECE).

the phase contrast imaging system. The normally line-integrated measurement is altered for the W7-X system to allow optical filtering, thereby providing radial resolution due to the pitch-angle variation of the magnetic field along the line-of-sight. Thus, density fluctuation measurements are possible on the outboard and inboard side with high fluctuation amplitude resolution of $\tilde{n}/n \leq 10\%$. Additionally, the wavenumber resolution can be tuned by variation of the beam diameter and can cover by design also the much smaller electron temperature gradient scale.

References

- [1] JENKO, F. et al., Phys. Plasmas **7** (2000) 1904.
- [2] HELANDER, P. et al., Plasma Phys. Control. Fusion **54** (2012) 1.
- [3] PROLL, J. H. E. et al., Phys. Rev. Lett. **108** (2012) 245002.
- [4] PROLL, J. H. E. et al., Plasma Phys. Controlled Fusion **58** (2016).
- [5] UMANSKY, M. V. et al., Contrib. Plasma Phys. **44** (2004) 182.